Available online at www.sciencedirect.com
ScienceDirect
C. R. Mecanique 336 (2008) 699–703
COMPTES RENDUS MECANIQUE
http://france.elsevier.com/direct/CRAS2B/

On the catastrophic bifurcation diagram of the truss arch system

Yannick G. Cantin [a], Nathalie M.M. Cousin-Rittemard [b,*], Isabelle Gruais [b]

[a] *Université de technologie de Belfort–Montbéliard, 90010 Belfort cedex, France*
[b] *I.R.M.A.R., Université de Rennes 1, campus de Beaulieu, 35042 Rennes cedex, France*

Received 6 May 2008; accepted after revision 7 July 2008

Available online 22 August 2008

Presented by Jean-Baptiste Leblond

Abstract

Non-linear physical models depend on parameters. One of the important basic issues of bifurcation theory is the determination of the fixed points of the system under investigation. Nevertheless, the branching of solutions rarely occurs in the real applications for which imperfections tend to distort these sharp transitions. In the present Note, the truss arch system is considered as a simple example of the coexistence of disjoint branches, even in a perfect case. Moreover, it is shown that the emergence of the subcritical bifurcations of the non-shallow configuration is the result of the connection of these disjoint branches. ***To cite this article: Y.G. Cantin et al., C. R. Mecanique 336 (2008).***

Résumé

A propos d'un diagramme de bifurcation catastrophique : le système de deux barres articulées. Les modèles des phénomènes physiques non linéaires dépendent de paramètres. Une première étape de la théorie des bifurcations est la détermination des points fixes du système étudié. Néanmoins, les intersections de branches de solutions sont rarement observées dans les applications réelles pour lesquelles des imperfections tendent à distordre ces transitions parfaites. Dans ce travail, le système plan de deux barres articulées, même sans imperfections, est considéré comme un exemple simple de coexistence de branches isolées pour une configuration géométrique large. De plus, on montre que l'émergence des bifurcations sous-critiques est le résultat de la connection de ces branches disjointes. ***Pour citer cet article : Y.G. Cantin et al., C. R. Mecanique 336 (2008).***

Keywords: Solids and structures; Bifurcation; Truss arch; Disjoint branch; Stability

Mots-clés : Solides et structures ; Bifurcation ; Barres articulées ; Branche disjointe ; Stabilité

* Corresponding author.
E-mail addresses: yannick.cantin@univ-rennes1.fr (Y.G. Cantin), nathalie.rittemard@univ-rennes1.fr (N.M.M. Cousin-Rittemard), isabelle.gruais@univ-rennes1.fr (I. Gruais).

1631-0721/$ – see front matter
doi:10.1016/j.crme.2008.07.001

1. Introduction

One of the important basic issues of bifurcation theory is the determination of the set of the fixed points of non-linear evolution equations as a function of their parameters. As a first approach, bifurcation theory may be seen as the study of the branching of solutions of a non-linear set of equations:

$$\mathbf{G}(\mathbf{U}, \Lambda) = 0 \tag{1}$$

where $\mathbf{U} \in \mathbb{R}^n$ and $\Lambda \in \mathbb{R}^p$ are the vectors of the unknowns and parameters, respectively and $\mathbf{G} : \mathbb{R}^n \times \mathbb{R}^p \to \mathbb{R}^n$ is a non-linear operator. From this point of view, the branching is described as a *perfect* bifurcation. In a larger parameter space, catastrophe theory reveals that such bifurcation points tend to occur as part of well-defined qualitative geometrical structures [1]. However, in many cases, bifurcation theory may a priori indicate that there are *disjoint* branches of solutions [2]. For example, the branching of solutions rarely occurs in the real applications for which imperfections tend to distort these sharp transitions [3]. The most complete set of the fixed points is thus desirable.

In the present paper, the perfect truss arch system is considered. It is a well known example of jump phenomena (see e.g. [4,5]). In order to carry out the set of the fixed points as comprehensively as possible, a unified computational approach is used. Starting from a known fixed point, a branch is carried out with Newton–Raphson algorithm with continuation (see e.g. [6–9]). The disjoint branches are reached using residue continuation [10,11]. The leading eigenvalues associated with the bifurcations and loss of stability are computed using QR algorithm (see e.g. [12]). The present work highlights that the perfect truss arch system is a simple example of coexistence of disjoint branches. Moreover, it is shown that the emergence of the subcritical bifurcations of the non-shallow configuration is the result of the connection of these disjoint branches.

2. Formulation

Let us denote E and A the Young moduli and the areas of the sections of the elastic rods of the truss arch system depicted in Fig. 1. Let (x_i, y_i) for $i = 1, 2, 3$, be the coordinates of the left and right hinge supports and of the upper point before loading $F = 0$. We denote by (x, y) the coordinates of the point 3 for a given vertical load $|F| > 0$. Without any loss of generality, we set: $x_3 = y_3 = 0$ and we note: $x_2 = a$, $x_1 = -a$, $y_1 = y_2 = h$. According to dimensional analysis (see e.g. [13]), we define the dimensionless unknowns and parameters:

$$\mathbf{U}(X \equiv x/h, Y \equiv y/h), \quad \Lambda(R \equiv a/h, f \equiv EAF/EA) \quad \text{and} \quad r = R^{-1}$$

The equilibria of the arches are the fixed points of the following dimensionless operator:

$$\mathbf{G}(\mathbf{U}, \Lambda) \equiv \begin{pmatrix} (\frac{1}{\hat{L}_1} - \frac{1}{L_1})(X + R) + (\frac{1}{\hat{L}_2} - \frac{1}{L_2})(X - R) \\ f + (\frac{1}{\hat{L}_1} - \frac{1}{L_1})(Y - 1) + (\frac{1}{\hat{L}_2} - \frac{1}{L_2})(Y - 1) \end{pmatrix} \tag{2}$$

where the dimensionless lengths of the rods at rest and for a given vertical load f respectively are:

$$L = L_1 = L_2 = \sqrt{R^2 + 1}, \quad \hat{L}_1 = \sqrt{(X + R)^2 + (Y - 1)^2}, \quad \hat{L}_2 = \sqrt{(X - R)^2 + (Y - 1)^2}$$

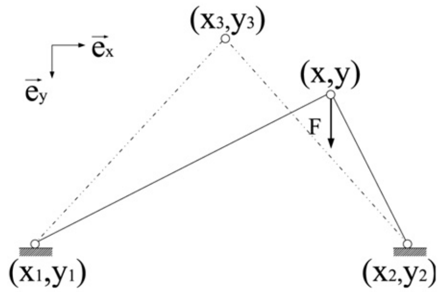

Fig. 1. The truss arch system.

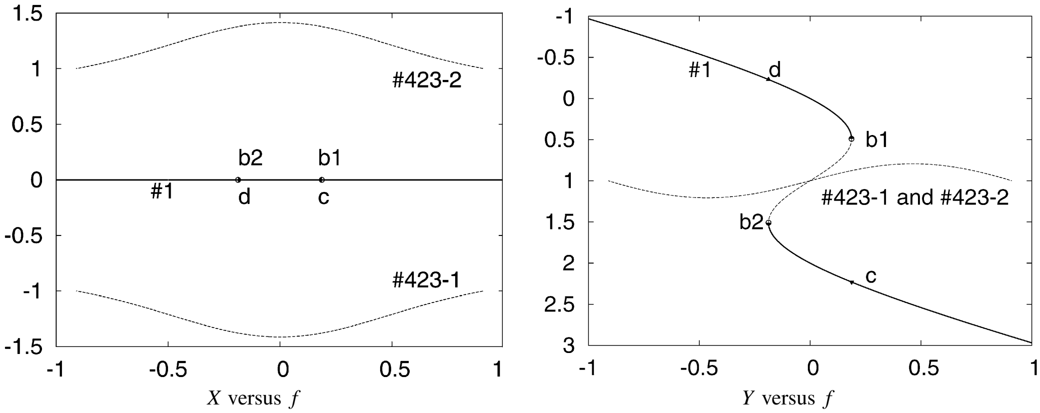

Fig. 2. Bifurcation diagram for an aspect ratio $r = 1$.

The system is conservative and the potential V is such that:

$$\forall K \in \mathbb{R}, \quad V(U, \boldsymbol{\Lambda}) = \sum_{i=1}^{2}\left(\frac{\hat{L}_i^2}{2L_i} - \hat{L}_i\right) - fY + K \tag{3}$$

3. Bifurcation diagrams

The response of the truss arch system depends on the aspect ratio $r \equiv h/a$. The bifurcation diagram of the shallow and non-shallow truss arches is carried out numerically [10,11].

3.1. Shallow truss arches

We first consider an aspect ratio equal to one (see Fig. 2). The solid and the dashed lines denote the stable and unstable parts of a branch respectively. For the latter case, only one real mode is stable. A critical load is labeled with the corresponding bifurcation name.

There is not one branch (see e.g. [14,11]) but three disjoint branches #1, #423-1 and #423-2.

Branch #1, along which $X = 0$, is the well known catastrophic snap-through phenomenon. Starting from rest ($f = 0$), the rods are compressed as a function of a vertical load. At the critical load f_{b1}, the saddle-node point $b1$ is eventually reached. The corresponding equilibrium is half-stable. The system snaps down towards the stable point c. From the equilibrium c, the decrease of the load yields to the critical value f_{b2}. Again, from the saddle-node $b2$, the system jumps up towards the stable equilibrium d leading to a hysteretic behavior as a function of the load f. Fig. 3 depicts the potential (3) maps in the vicinity of three points along Branch #1. Point $b1$ is half stable in Y direction. This energy point of view illustrates that the snap through is perfectly vertical.

Branches #423-2 and, symmetrically, #423-1 are unstable. They straddle the *horizontal line* between the hinge supports: $Y = 1$. The coordinates of the fold points are ($X = \pm 1.41 = \pm L$, $Y = 1$) where $L = L_1 = L_2$. At rest ($f = 0$), the two rods are horizontal. An unstable equilibrium is possible if the left rod is in traction while the right one is compressed, and symmetrically.

3.2. Non-shallow truss arches

Fig. 4 depicts the evolution of Branch #423-2 as a function of the aspect ratio r within the range $[0.9, 2.5]$. As the aspect ratio increases, the curve #423-2 (symmetrically #423-1) tends to Branch #1. Eventually, for $r = 2.398 \sim 2.4$, the disjoint Branches #423-2 and #423-1 both connect on Branch #1 through two cusps. The corresponding graphs are marked with a dashed dotted curve in Fig. 4. This critical value of the aspect ratio is the threshold between shallow and non-shallow truss arch system. The connection of Branches #423-2 and #423-1 gives rise to the three unstable branches #4, #2 and #3 and the four corresponding subcritical bifurcations. Branch #2 emerges as the result of the collapse of Branches #423-1 and #423-2 turning round the hinge supports i.e. #2 = #2-1 ∪ #2-2. Branch #3 (resp. #4)

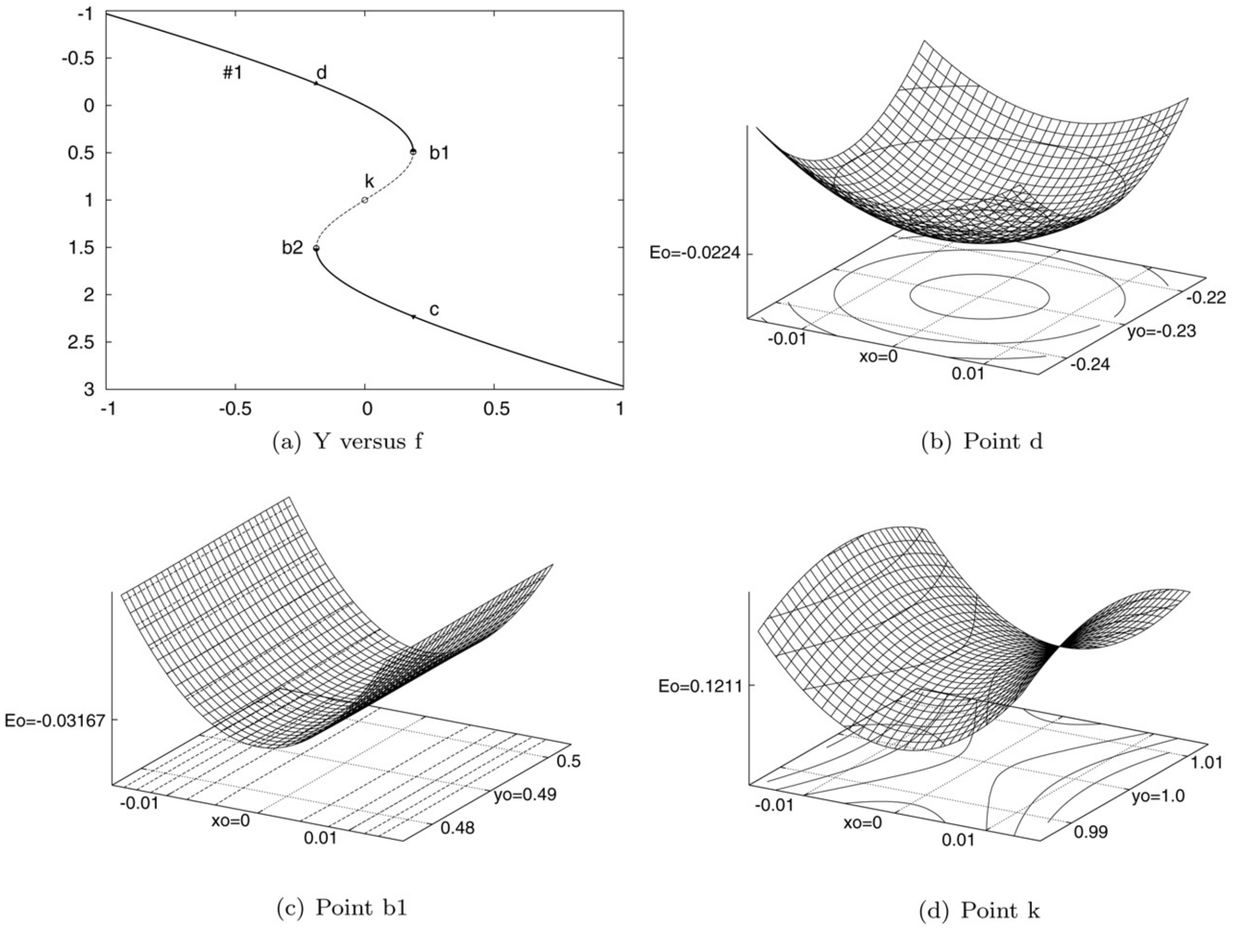

Fig. 3. Branch #1 for $r = 1$: in (a), Y as a function of the load parameter f is plotted while (b)–(c)–(d) depict the potential (3) maps as functions of X and Y in the vicinity of the equilibria d, $b1$ and k of the bifurcation diagram (a) are shown. The mesh unit is equal to 10^{-3}.

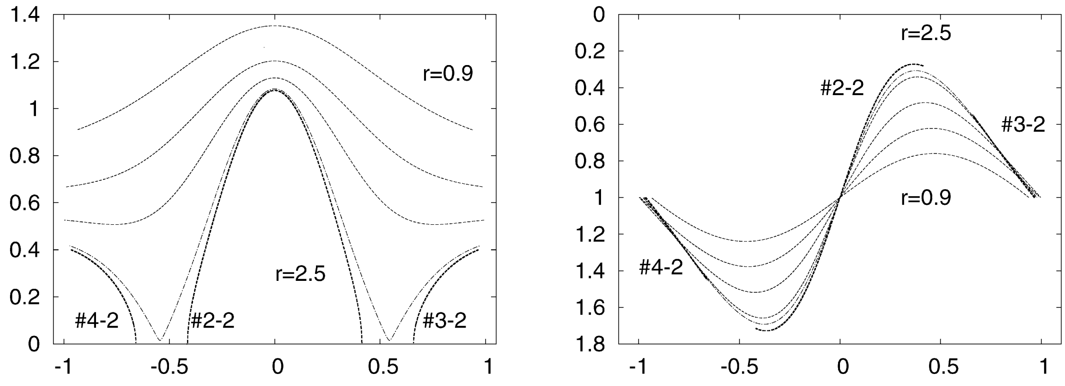

Fig. 4. Shallow truss arches evolution of Branch #423-2 for $r \in [0.9, 2.5]$: in (a) and (b), X and Y are plotted versus the load f respectively. The increment of the aspect ratio between two dashed curves is 0.4. For emphasis, bold dashed curve is used for $r = 2.5$. The dashed dotted linestyle is used for $r = 2.39 \sim 2.4$.

is the result of the connection of Branches # 423-1 and #423-2 for which $f > 0$ (resp. $f < 0$) turning towards the hinge supports i.e. #3 = #3-1 ∪ #3-2 (resp. #4 = #4-1 ∪ #4-2). We denote $s2$ and $s1$ the branching between Branches #4 and #3 with Branch #1 respectively and $r2$ and $r1$ the intersections between Branches #2 and #1.

Above the critical threshold, the perfect vertical snap-through would not be observed. Indeed, Branch #1 becomes unstable at the subcritical bifurcation $r1$, that is before the saddle-node bifurcation $b1$. While turning, the system snaps down to the stable point c. From the equilibrium c, the decrease of the load yields to the critical value $f = -f_c$. Again, from the subcritical $r2$, the system jumps up to the stable equilibrium d while turning. The vertical snap through with rotation appears as an hysteresis phenomenon as a function of the load f.

As the aspect ratio tends towards infinity, the model (2) degenerates:

$$X\left(\left(X^2 + (Y-1)^2\right)^{-1/2} - 1\right) = 0 \tag{4a}$$

$$(Y-1)\left(\left(X^2 + (Y-1)^2\right)^{-1/2} - 1\right) + \frac{f}{2} = 0 \tag{4b}$$

For all $X \neq 0$, X and Y are related to each other by a circle equation minus a point at rest ($f = 0$), that is Branch #2:

$$X^2 + (Y-1)^2 = 1$$

For $X = 0$, Eq. (4b) is reduced to the two half straight lines denoted, that is branch #1:

$$Y = 1 + \operatorname{sign}(Y-1) - \frac{f}{2}$$

Also, if $Y = 1$ then Eq. (4a) is reduced to the two points ($X = \pm 1,\ Y = 1$) at rest.

4. Conclusion

The snap buckling of the elastic rods or shells are well known examples of jump phenomena (see e.g. [4,5]). The present work highlights that the perfect truss arch system is a simple example of coexistence of disjoint branches reached with an ad-hoc numerical method [10,11]. Moreover, it is shown that the emergence of the subcritical bifurcations corresponding to the snap-through turning round and towards the hinge supports of the non-shallow configuration is the result of the connection of disjoint branches.

References

[1] R. Thom, Structural Stability and Morphogenesis, Addison-Wesley, 1989, p. 404.

[2] M. Golubitsky, D. Shaeffer, Singularities and Groups in Bifurcation Theory: I, Applied Mathematical Sciences, vol. 51, Springer-Verlag, 1985, p. 463.

[3] B.J. Matkowsky, E.L. Reiss, Singular perturbations of bifurcations, SIAM J. Appl. Math. 33 (1977) 230–255.

[4] Q.S. Nguyen, Stability and Nonlinear Solid Mechanics, John Wiley, 2000, p. 398.

[5] S.S. Antman, Non-Linear Problems of Elasticity, Springer, 2005, p. 831.

[6] E.L. Allgower, K. Georg, Numerical path following, in: P.G. Ciarlet, J.L. Lions (Eds.), Handbook of Numerical Analysis, vol. 5, 1997, pp. 3–208, 818.

[7] E. Doedel, L.S. Tuckerman, Numerical Methods for Bifurcation Problems and Large-Scale Dynamical Systems, IMA Volumes in Mathematics and Its Applications, vol. 119, Springer, 2000, p. 471.

[8] H. Dang-Vu, C. Delcarte, Bifurcations et chaos, Ellipses, 2000, p. 447.

[9] Iu.A. Kuznetsov, Elements of Applied Bifurcation Theory, Applied Mathematical Sciences, vol. 112, Springer-Verlag, 2004, p. 631.

[10] I. Gruais, N.M.M. Cousin-Rittemard, H.A. Dijkstra, A priori estimation of a global Homotopy Residue Continuation method, Numerical Functional Analysis and Optimization 26 (4–5) (2005) 507–521.

[11] N.M.M. Cousin-Rittemard, I. Gruais, Continuation methods and disjoint equilibria, Revue Roumaine de Mathématiques Pures et Appliquées 52 (1) (2007) 9–34.

[12] G.H. Golub, C.F. Van Loan, Matrix Computations, Johns Hopkins Studies in Mathematical Sciences, 1996, p. 694.

[13] G.I. Barenblatt, Scaling, Cambridge University Press, 2003, p. 171.

[14] K. Ikeda, K. Murota, Imperfect Bifurcation in Structures and Materials, Applied Mathematical Sciences, vol. 149, Springer-Verlag, New York, 2002, p. 411.